Fibers and Polymers 2015, Vol.16, No.1, 138-145
DOI 10.1007/s12221-015-0138-2

ISSN 1229-9197 (print version)
ISSN 1875-0052 (electronic version)

Dynamic Mechanical and Impact Properties of Composites Reinforced with Carbon Nanotubes

V. Obradović*, D. B. Stojanović, I. Živković, V. Radojević, P. S. Uskoković, and R. Aleksić

University of Belgrade, Faculty of Technology and Metallurgy, Belgrade 11120, Serbia
(Received February 19, 2014; Revised August 27, 2014; Accepted September 1, 2014)

Abstract: This study presents dynamic mechanical and impact properties of the new form of hybrid thermoplastic composites. The six composites of polyurethane/*p*-aramid multiaxial fabric forms (Kolon fabrics) were impregnated with 10 wt% poly(vinyl butyral) (PVB)/ethanol solution with the addition of pristine multiwalled carbon nanotubes (MWCNT) where the PVB/fabric ratio was 20 wt%. All the composites consisted of four layers of the impregnated fabrics. The MWCNT/PVB content was 0, 0.5 and 1 wt%. The surface of the three composites with different MWCNT/PVB content was modified with γ-aminopropyltriethoxy silane (AMEO silane)/ethanol solution. The physical and dynamic mechanical properties of the prepared composite samples were analyzed by dynamic mechanical analysis (DMA) and high speed puncture impact tester. The structures of the composite samples were investigated by scanning electron microscopy (SEM). The results showed that the Kolon/AMEO/PVB/1 wt% MWCNT sample yielded a 60 % improvement in the storage modulus and a 73 % improvement in the impact absorbed energy compared to the Kolon/PVB sample. The carbon nanotubes (MWCNT) were added to improve the dynamic mechanical and impact properties of the materials for ballistic protection.

Keywords: Kolon fabrics, Multiwalled carbon nanotubes, γ-aminopropyltriethoxy silane, Dynamic mechanical analysis, Puncture impact test

Introduction

Two main ways are important for the achievement of polymer composites with improved properties due to the addition of carbon nanotubes (CNTs): proper interfacial interaction between nanotubes and polymer by increasing the surface roughness or the surface reactivity of CNTs as well as their good dispersion in the polymer matrix [1,2]. Pristine CNTs are usually not well dispersed in different polymer matrices due to the strong Van der Waals attractive forces between nanotubes which tend to their agglomeration. Small amounts of CNTs in polymer matrices are easier dispersed and it is assumed that the modulus is improved. In contrary to that, when the concentration of CNTs becomes large, the nanotubes can interact and may form small aggregates, which restrict the interfacial contact area for stress transfer in the polymer matrix [1]. The area becomes imperfect and it can seriously reduce the effective stiffness and strength of the composite [3]. In fact, dispersion presents a balance between the forces of attraction among the nanotubes and the stabilizing network created by the presence of matrix. The strength of such a dynamic complex is guided by temperature, viscosity and formation of bonding between the filler surface and the matrix [4]. Compatibility with the polymer matrix can be maintained by chemical modification of CNTs, which tend to agglomerate due to presence of Van der Waals forces between their polarizable π-electron systems. Solvents, surfactants, strong acids, noncovalent and covalent bonding and other chemical methods are used for surface modification of the CNTs surface and homogeneous dispersion of carbon nanomaterials in water and various polymer matrix materials [5-7]. There is a certain difficulty with adsorbed molecules, which form the strong bonds to CNTs because all moduli decrease due to great changes in the lattice constant and radius [8]. Ionic modification through common electrostatic attraction of cation-π or π-π systems between the modifier and CNTs reduces the Van der Waals forces and leads to dispersion of nanotubes [9].

Carbon nanotubes possess light-weight and excellent energy absorption capacity and thus are applied in manufacturing antiballistic materials for bulletproof vests, explosion-proof blankets, body and vehicle armors. One study shows that the carbon nanotube body armor can withstand high bullet speed and have a constant ballistic resistance even when bullets strike at the same point [10,11].

Composite structures are disclosed to various impact loading conditions and when they are not constructed properly, they can endure catastrophic failure. There are two types of impact damages on composite structures - complete penetration of the laminate by high-velocity ballistic impacts like low-mass projectiles and non-penetrating impacts by low-velocity impacts, like liquid jet or wind trash strikes [12]. Matrix cracks which appear at the interfaces between layers cause internal delamination in composites after impact loading. Low velocity impacts can weaken the laminate stiffness due to the piled delaminations, which are created by impact loading along laminate thickness [13]. The fracture does not occur on a single hit with low energy impact process, which is called subperforation, and thus is related to all the impact events with deficient velocity and kinetic energy which are not enough to provoke a penetration. Still, the certain damage can be obtained by repeated impacts

*Corresponding author: vobradovic@tmf.bg.ac.rs

even when the impact energy is very low [14]. The total impact energy is a sum of crack initiation energy and crack spreading (propagation) energy. The fragile materials possess high values of the crack initiation energy and low values of the crack spreading energy, while the tough materials are characterized by low breakage initiation energy and high breakage spreading energy [15].

In recent years, *p*-aramid fabrics have been increasingly applied to various composite structures for body armor in ballistics. Their excellent mechanical properties are obtained from the long, straight fibers of poly(paraphenylene terephthalamide). The fabrics containing *p*-aramid fiber have a tensile strength-to-weight ratio 5 times higher than steel of an equal weight basis. They provide great heat resistance. Beside their application in ballistics, they have been utilized as hoses, tires, heat protection products and composites [16,17]. Poly(vinyl butyral) (PVB) is a flexible and industrially significant polymer, which is produced from condensation of poly(vinyl alcohol) (PVA) with n-butyraldehyde in an acid environment. This polymer possesses high impact strength at low temperatures, high impact energy absorption and excellent adhesive properties with a variety of materials (like glass, metals and plastics). About 65 % of all PVB polymers are utilized in automobile industry to ensure safety in glass laminates [18].

In this study, the pristine multiwalled carbon nanotubes (MWCNT) were used to improve dynamic mechanical properties of materials for ballistic protection. The composites of polyurethane/*p*-aramid multiaxial fabric forms (Kolon fabrics) were coated with MWCNT/PVB ethanol solution. The surfaces of one part of the polyurethane/*p*-aramid multiaxial fabric composites were modified with γ-aminopropyltriethoxysilane (AMEO silane)/ethanol solution. The dynamic mechanical and impact properties of the prepared composites (which are mainly used for bulletproof vests) were analyzed by the dynamic mechanical analysis (DMA) and high speed puncture impact tester.

Experimental

Materials

A polymer powder poly(vinyl butyral) (Mowital B60H, Kuraray Specialities Europe) and absolute ethanol (Zorka Pharma, Šabac) were used for preparing the PVB solution and the carbon nanotubes, MWCNT (Cheap Tubes Inc., USA), were added into the PVB solution. The nanotubes lengths were from 3 μm to 30 μm with the outer diameters from 13 nm to 18 nm. Multiaxial aramid fabrics (Martin Ballistic Mat, Ultratex, Serbia) with the *p*-aramid fiber type Kolon (Heracron, Kolon Industries, Inc., Korea) were used. Each fabric contained fiber knitting with four different angle orientations: +45°, 0°, 90° and -45° (data provided by Martin Ballistic Mat). The fibers were impregnated with polyurethane film inside (Desmopan, Bayer) and fastened together with a light-weight polyester thread (Korteks, Turkey) [16]. One layer of the Kolon fabric consisted of 95 wt% of aramid and 5 wt% of polyurethane.

Dynasylan® AMEO, γ-aminopropyltriethoxysilane ($(C_2H_5O)_3SiC_3H_6NH_2$), Degussa-Evonik) was applied to the process of the surface modification of the fabrics.

Preparation of the Hybrid Composites

For this study, six composite configurations were fabricated by hot compression. Each composite configuration consisted of four impregnated layers of the Kolon fabrics. The four impregnated multiaxial fabric layers were placed, each layer on the previous one, keeping the same fiber knitting angle orientations (+45°, 0°, 90° and -45°) with the same direction of the polyester thread seams.

The weight of the four Kolon fabric layers was 40 g and the pre-defined PVB/fabric ratio for the impregnation was 0.2 (20 wt% of PVB, 8 g). The designation and preparation of the composite configuration are presented in Table 1. For the three composites, the fabrics were firstly coated with AMEO silane/ethanol solution due to the surface modification of the fabrics. The modification of these composite configurations was managed by impregnation with 2 wt% AMEO silane/ethanol solution. The solution was stirred for ten minutes on a magnetic stirrer for the hydrolysis of AMEO silane. After the impregnation, the fabrics were left to dry for 24 hours.

Then, the experiments were carried out with the 10 wt% PVB/ethanol solution. At first, the MWCNT were added into ethanol with concentration of 0.5 and 1.0 wt% in regard to PVB, where MWCNT/PVB ratio was 0.005 and 0.01, respectively. This solution was ultrasonicated for 30 minutes

Table 1. The designation and preparation of the hybrid composites

No.	Designation of composite	Composite preparation
1	Kolon/PVB	The sample impregnated with PVB solution
2	Kolon/AMEO/PVB	The sample impregnated with AMEO silane and PVB solutions
3	Kolon/PVB/0.5 wt% MWCNT	The sample impregnated with 0.5 wt% MWCNT/PVB solution
4	Kolon/PVB/1 wt% MWCNT	The sample impregnated with 1 wt% MWCNT/PVB solution
5	Kolon/AMEO/PVB/0.5 wt% MWCNT	The sample impregnated with AMEO silane and 0.5 wt% MWCNT/PVB solutions
6	Kolon/AMEO/PVB/1 wt% MWCNT	The sample impregnated with AMEO silane and 1 wt% MWCNT/PVB solutions

separately in order to provide satisfying dispersion of the carbon nanotubes. After the dispersion process, the ethanol-MWCNT mixture was put into the 20 wt% PVB/ethanol solution in order to achieve final concentration for the 10 wt% PVB/ethanol solution. The solution was then mixed on a magnetic stirrer overnight. Afterwards, MWCNT were separated and well-dispersed in PVB/ethanol solution, which was stable in a long term. After certain period of similarity between the PVB solution with MWCNT and the ethanol-MWCNT mixture, MWCNT formed residual deposits at the flask bottom after one month [19].

All the composites were impregnated with 80 g PVB/ethanol solution (72 g of ethanol and 8 g of PVB) and appropriate MWCNT concentration (0, 0.5 or 1.0 wt% with regard to PVB). It was the impregnation of both sides of the fabrics with the appropriate solutions that led to obtaining all the composite fabrics, after which they were left to stay for 24 hours for ethanol evaporation. They were processed in the compress machine (N 840 D Hix Digital Press) at a temperature of 170 °C under a pressure of 3 bar for 15 minutes. Next, the composite fabrics were turned on the back-side and pressed additionally for 15 minutes under the same conditions. After the compression, the dimensions of all the composite samples were 150 mm×150 mm, with the thickness of 2.1 mm. The samples of appropriate sizes were cut from the composites (the cut directions were 0 ° and 90 ° fiber angle orientations) and they were used for the further characterizations - dynamic mechanical analysis, scanning electron microscope analysis and impact tester analysis.

Characterization

Dynamic mechanical thermal analysis (DMA, Q800 TA Instruments, USA) for the Kolon fabrics was carried out in a dual cantilever mode at a frequency of 1 Hz where the temperature ranged from 40 °C to 170 °C with a heating rate of 3 °C/min in nitrogen atmosphere for the determination of the storage modulus (*E′*). The dimensions of the samples for this analysis were 60 mm×13 mm×2.1 mm and they were cut parallel to the polyester thread seams (90 ° fiber angle orientation) with respect to their length. The two samples from each type of the composites were tested with a relative error of 3 %.

The samples for the impact tests had a square shape, with the dimensions of 60 mm×60 mm and the thickness of 2.1 mm. There were four tests per one composite type. The tests were conducted on a high speed puncture impact testing machine Hydroshot HITS-P10 Shimadzu, Japan. This machine can operate at speeds up to 20 m/s and temperature range from -40 °C to 150 °C. In this work, the inner diameter of the clamping plates which gripped the samples was 40 mm. The tip of the striker was a hemisphere with the diameter of ϕ=12.7 mm. The puncture velocity was 2 m/s, and the experiment was carried out at room temperature. The load, energy, velocity, displacement and time data are available from Data Processing Software. The impact testing device used in this work is displayed in Figure 1.

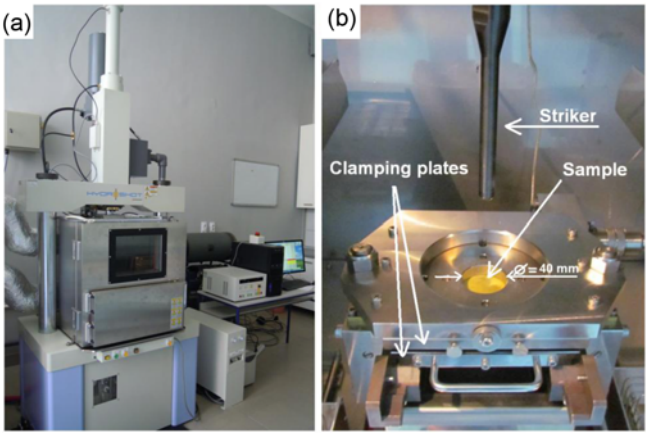

Figure 1. (a) High speed puncture impact tester set-up and (b) striker and clamping plates inside impact tester.

The images of samples after the impact test were taken using a scanner (HP Scanjet) to obtain their high-scans (scan picture option, 600 dpi resolutions), which were treated by image analysis software. The image analyses for prints of the damaged areas were performed in Image Pro-Plus software by converting the images in grayscale mode and transferring them to bitmap analyses. Bitmap analysis enables to visualize the print of the impact area using the special calibrations for converting intensity and pixel position data to millimeter scale data.

The surface of the samples was vacuum-coated by evaporation with gold and observed under a scanning electron microscope (SEM) JEOL JSM 6610, operated at 15 kV.

Results and Discussion

Dynamic Mechanical Analysis (DMA)

The results of DMA are presented in Figure 2. These results revealed that the modulus (*E′*) of Kolon/PVB sample increased with the surface modification of fabrics and content of multiwalled carbon nanotubes. The introduction of MWCNT to untreated fabrics (Kolon/PVB) increased the storage modulus by 26.6 % for the Kolon/PVB/0.5 wt% MWCNT and by 21.2 % for the Kolon/PVB/1 wt% MWCNT sample at 40 °C (Figure 2, Table 2). These values indicate that a good dispersion of MWCNT was gained more with the 0.5 wt% than with the 1 wt%. The impregnation of Kolon fabrics with AMEO silane maximized the storage modulus for all the samples due to the strong bonds between AMEO silane and Kolon/PVB surface with a good distribution of MWCNT. For the Kolon/AMEO/PVB sample the storage modulus was 1690 MPa, higher than that for the Kolon/PVB sample (1377 MPa). The storage modulus value for the Kolon/AMEO/PVB/0.5 wt% MWCNT sample increased by

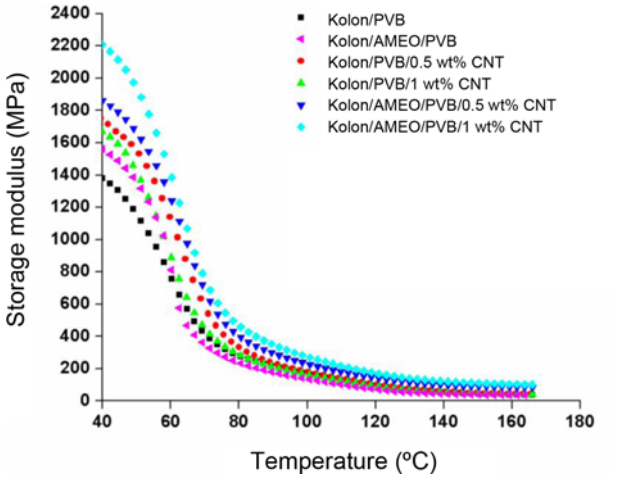

Figure 2. Storage modulus for all the samples.

Table 2. DMA test results for all the samples

No.	Composite	E' (40 °C, MPa)	T_g (°C) (Onset point)
1	Kolon/PVB	1377	70.52 °C
2	Kolon/AMEO/PVB	1690	72.49 °C
3	Kolon/PVB/0.5 wt% MWCNT	1744	70.63 °C
4	Kolon/PVB/1 wt% MWCNT	1669	74.30 °C
5	Kolon/AMEO/PVB/0.5 wt% MWCNT	1853	70.90 °C
6	Kolon/AMEO/PVB/1 wt% MWCNT	2204	74.53 °C

34.6 % and for the Kolon/AMEO/PVB/1.0 wt% MWCNT sample it was enhanced by 60.0 % in comparison with Kolon/PVB respectively.

The glass transition temperature, T_g, was determined from the onset point of storage modulus curve. The T_g value for the Kolon/PVB sample was 70.52 °C, and the values for the samples with the content of MWCNT 0.5 wt% and 1.0 wt% were 70.63 °C and 74.30 °C, respectively (Figure 2, Table 2). It is obvious that, even in the absence of specific interactions with the polymer, the particles behaved as functional physical cross-links, and thus reduced the overall mobility of the polymer chains. After modification with AMEO silane, the storage modulus increased considerably and T_g rose slightly. The values of T_g were 70.90 °C and 74.53 °C for the Kolon/AMEO/PVB/0.5 wt% MWCNT and the Kolon/AMEO/PVB/1.0 wt% MWCNT samples, respectively.

Impact Tester Analysis

During the impact process the complete penetration of the samples did not occur, and they were deformed after the test. It was a good opportunity to analyze the deformation and energy absorption during the impact. Generally, the impact energy is absorbed for creating elastic and plastic deformations

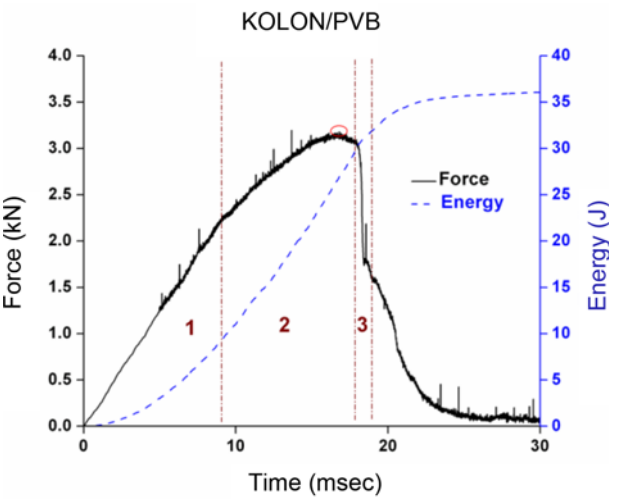

Figure 3. Impact test results for the Kolon/PVB sample.

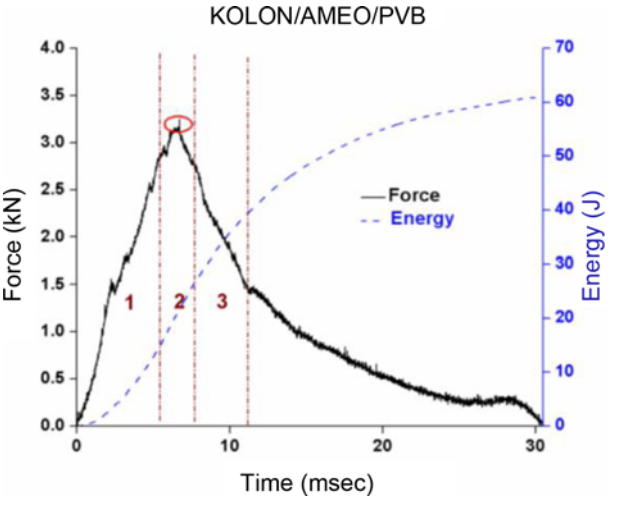

Figure 4. Impact test results for the Kolon/AMEO/PVB sample.

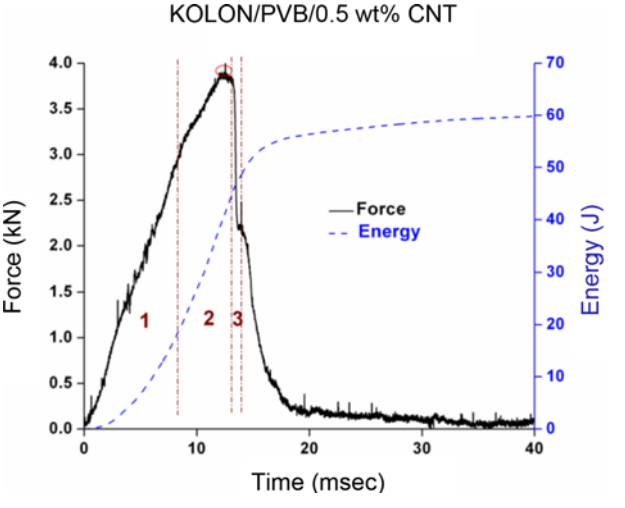

Figure 5. Impact test results for the Kolon/PVB/0.5 wt% CNT sample.

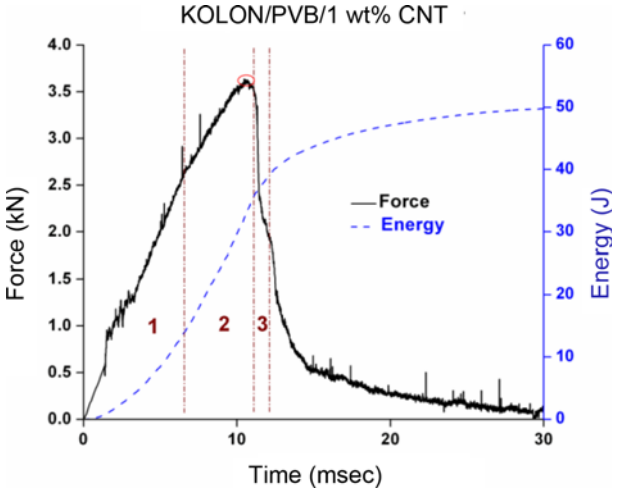

Figure 6. Impact test results for the Kolon/PVB/1 wt% CNT sample.

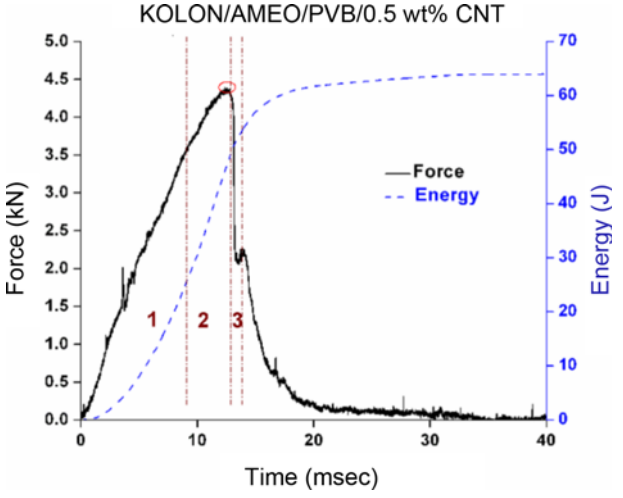

Figure 7. Impact test results for the Kolon/AMEO/PVB/0.5 wt% CNT sample.

along with failure modes. For the composite materials, the total impact energy is converted to elastic deformation and damage modes since there is no plastic deformation [20]. In this study, absorbed energy is responsible for the energy

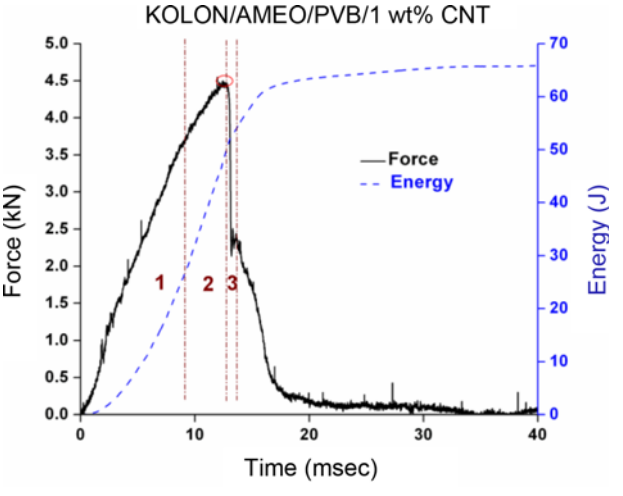

Figure 8. Impact test results for the Kolon/AMEO/PVB/1 wt% CNT sample.

spent in producing damage.

The most remarkable impact test results are presented in Figures 3-8 with the force-time-energy dependencies marked by the three energy absorption zones [21,22]. Zone 1 is defined as elastic zone which is linear, with elastic deformation of all the layers caused by absorbed impact energy of a striker. Zone 2 presents a slippage/breakage zone, while Zone 3 is a failure zone. The slippage and delamination of composites start in Zone 2 and thus the slope of the force curve is changing. The beginning of Zone 3 is characterized by a sudden drop in force and the end of this zone is noted by a specific shape of a force curve which identifies the failure of composites.

The appropriate standard deviations of the maximal impact force and the total energy absorbed for each type of the samples are presented in Table 3. The value of the maximum force, F_{max}, for the Kolon/PVB sample was 3.13 kN and it was increasing with the addition of 0.5 wt% MWCNT (3.94 kN) while it was decreasing for the sample with 1 wt% MWCNT (3.64 kN) due to incomplete distribution and deagglomeration of MWCNT. This phenomenon can be corrected by surface modification of fabrics with AMEO silane since F_{max} for the AMEO modified samples increased

Table 3. Impact test results for all the samples

No.	Composite	F_{max} (kN)	Total energy absorbed (J)	Energy absorbed in Zone 1 (J)	$(E_{z1}/E_{abs}\times100)$ (%)	Slope (kN/mm)
1	Kolon/PVB	3.13 (0.58*)	37.97 (8.02*)	9.08	24	0.21
2	Kolon/AMEO/PVB	3.25 (0.28*)	60.89 (8.85*)	14.90	24	0.24
3	Kolon/PVB/0.5 wt% MWCNT	3.94 (0.37*)	55.03 (3.79*)	18.39	33	0.24
4	Kolon/PVB/1 wt% MWCNT	3.64 (0.23*)	49.94 (2.55*)	13.60	27	0.22
5	Kolon/AMEO/PVB/0.5 wt% MWCNT	4.40 (0.26*)	63.91 (8.86*)	25.80	40	0.26
6	Kolon/AMEO/PVB/1 wt% MWCNT	4.55 (0.31*)	65.69 (5.79*)	26.71	41	0.37

*Standard deviation.

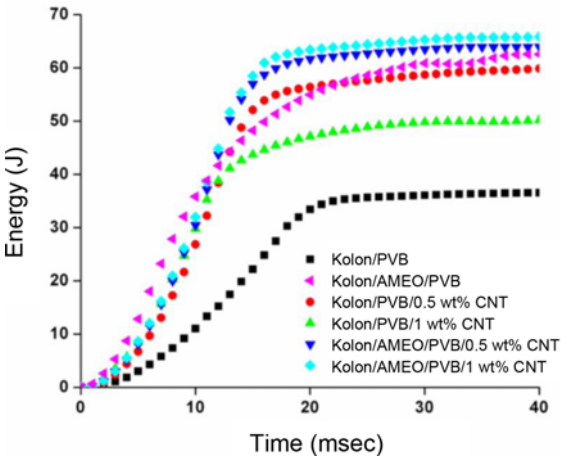

Figure 9. Energy absorption graph for all the samples.

- for the Kolon/AMEO/PVB was 3.25 kN. This trend is also observed for the modified ones with 0.5 wt% and 1 wt% MWCNT (4.40 kN and 4.55 kN, respectively). These results were in coherence with the results for the storage modulus from DMA analysis and they demonstrated the influence of the modification and MWCNT content on the dynamic mechanical and impact properties of the composite samples.

The values for the absorbed energy had a similar trend and they are presented in Table 3, with the values of the total absorbed energy (E_{abs}), the energy absorbed in Zone 1 (E_{z1}) and the percentage of this energy ($E_{z1}/E_{abs}\times100$). It can be observed that with the addition of MWCNT, the percentage of the energy in Zone 1 was increasing (this Zone became wider), and this effect was more noticeable with the AMEO modification. The linear slope of the force-displacement curve in the elastic zone was obtained by Data Processing Software. This slope is proportional to modulus of elasticity [23] and it was increasing with the addition of 0.5 wt% MWCNT, decreasing with 1 wt% MWCNT and increasing again with AMEO silane surface modification.

The AMEO modified samples displayed greater absorbed energy compared to the unmodified ones with the same content of MWCNT (Figure 9, Table 3). The result for the Kolon/AMEO/PVB/1 wt% MWCNT sample produced around 73 % improvement in the impact energy absorption (65.69 J) compared to the Kolon/PVB sample (37.97 J). Some authors have observed and concluded that the maximum load increases with the increasing of the impact absorbed energy [24].

Print Analysis

The scanned images of the impacted samples were analyzed in Image Pro-Plus software and they present the projections of the deformed samples. The images are depicted in Figures 10(a) and 11(a). The dimensions of the inspected zones were 50 mm×50 mm, and they contained the completed samples after the impact tests. The print analyses of these images,

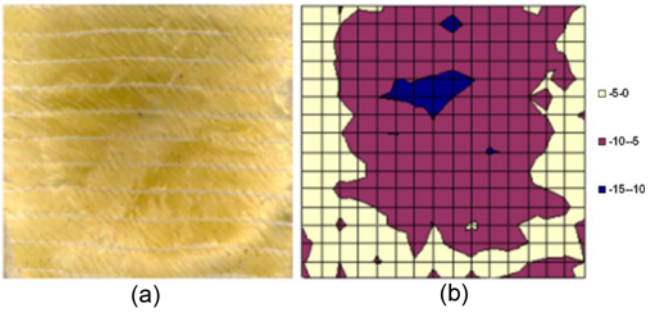

Figure 10. (a) Scanned image and (b) print analysis for the Kolon/PVB sample.

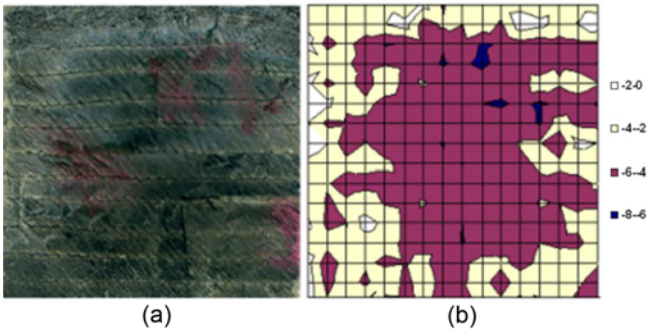

Figure 11. (a) Scanned image and (b) print analysis for the Kolon/AMEO/PVB/1 wt% MWCNT sample.

with the millimeter scale legends, for the Kolon/PVB (No.1) and the Kolon/AMEO/PVB/1 wt% MWCNT (No. 6) samples are given in Figures 10(b) and 11(b). The deepest points for their concavities after the impact tester analysis were 13 mm (No.1) and 7.1 mm (No.6). According to the references [25-27], the dark blue color represents the main damage areas and the quotient between the sum of these areas and the inspected square area (2500 mm^2) was measured in Image-Pro Plus software. The main damage areas are larger within the Kolon/PVB sample around 433 % compared to the Kolon/AMEO/PVB/1 wt% MWCNT sample. The Kolon/PVB sample had a concave penetration shape after the impact test, while the Kolon/AMEO/PVB/1 wt% MWCNT sample had a flat surface strain due to the impact stress dispersion into wider region. These deformations in the surface shapes of the samples and their difference in the depth approve that the AMEO modification and addition of MWCNT in the composite improved its mechanical properties.

SEM

The appropriate SEM images of the composite samples, with different magnification, are depicted in Figure 12: a) Kolon/PVB, b) Kolon/AMEO/PVB/1 wt% MWCNT, c) Kolon/PVB/1 wt% MWCNT (scale bar 10 μm for the three of them) and d) Kolon/AMEO/PVB/1 wt% MWCNT (scale bar 1 μm). From Figure 12(a) the PVB aggregates are visible

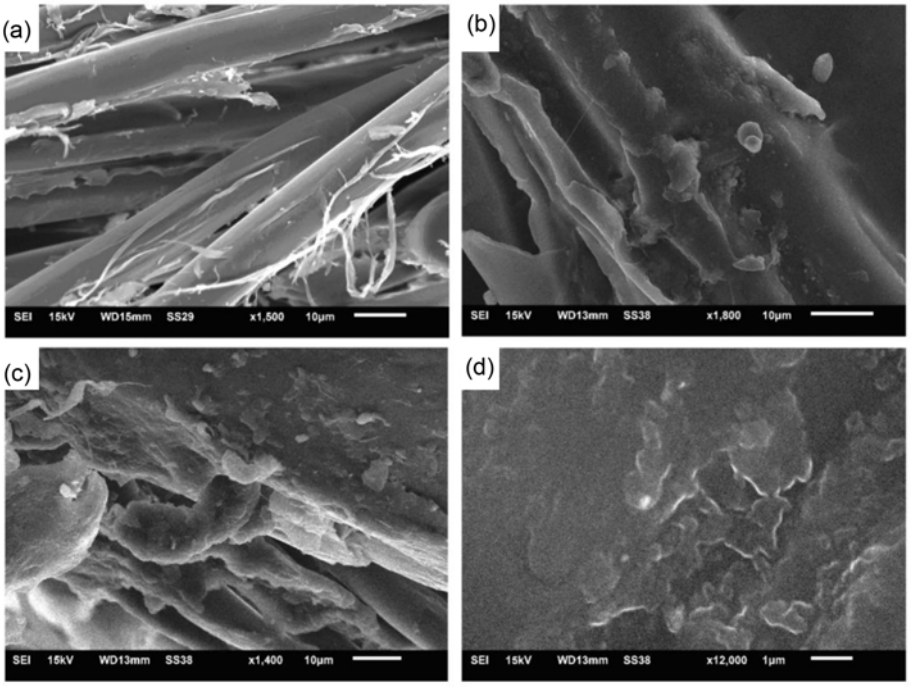

Figure 12. SEM images of (a) the Kolon/PVB sample, (b) the Kolon/PVB/1 wt% MWCNT sample, and the Kolon/AMEO/PVB/1 wt% MWCNT sample (c and d).

beside the Kolon fibers, while in Figures 12(b), 12(c) and 12(d) the small MWCNT bundles are present. The smallest diameter of the MWCNT agglomerates is about 200 nm.

Conclusion

The dynamic mechanical and impact properties of the prepared composites were studied by DMA and high speed puncture impact tester analysis. During the impact test, the penetration of the samples did not appear. The increases of storage modulus, impact force and absorbed energy were achieved by addition of MWCNT and impregnation of polyurethane/*p*-aramid multiaxial (Kolon) fabrics with AMEO silane probably as a consequence of strong bond formation between AMEO silane and thermoplastic polymers and additionally due to favorable dispersion of carbon nanotubes. The best results of the DMA analysis and impact test were achieved with the greatest concentration of MWCNT (1 wt%) and the surface modification with AMEO silane. The results for the storage modulus from DMA analysis and the maximum force from impact tester analysis were in coherence and they indicated that surface modification of Kolon fabrics and MWCNT content enhanced the dynamic mechanical and impact properties of the composites.

Acknowledgements

The authors wish to acknowledge the financial support from the Ministry of Education, Science and Technological Development of the Republic of Serbia through Project Nos. TR 34011 and III 45019.

References

1. M. R. Loos, V. Abetz, and K. Schulte, *J. Polym. Sci. Pol. Chem.*, **48**, 5172 (2010).
2. J. P. Salvetat, J. M. Bonard, N. H. Thomson, A. J. Kulik, L. Forró, W. Benoit, and L. Zuppiroli, *Appl. Phys. A-Mater. Sci. Process.*, **69**, 255 (1999).
3. P. Barai and G. J. Weng, *Int. J. Plast.*, **27**, 539 (2011).
4. A. Godara, L. Mezzo, F. Luizi, A. Warrier, S. V. Lomov, A. W. van Vuure, L. Gorbatikh, P. Moldenaers, and I. Verpoest, *Carbon*, **47**, 2914 (2009).
5. M. M. Tomishko, O. V. Demicheva, A. M. Alekseev, A. G. Tomishko, L. L. Klinova, and O. E. Fetisova, *Russ. J. Gen. Chem.*, **79**, 1982 (2009).
6. S. Parveen, S. Rana, and R. Fangueiro, *J. Nanomater.*, ID 710175 (2013).
7. H. Kwon, S. Cho, M. Leparoux, and A. Kawasaki, *Nanotechnology*, **23**, 225704 (2012).
8. K. Z. Milowska and J. A. Majewski, *Phys. Chem. Chem. Phys.*, **15**, 14303 (2013).
9. S. B. Jagtap and D. Ratna, *J. Appl. Polym. Sci.*, **130**, 2610 (2013).
10. K. Mylvaganam and L. C. Zhang, *Nanotechnology*, **18**, 475701 (2007).

11. A. Morka and B. Jackowska, *Comput*. *Mater*. *Sci*., **50**, 1244 (2011).
12. E. Sevkat, B. Liaw, F. Delale, and B. B. Raju, *Compos*. *Pt. B-Eng*., **41**, 403 (2010).
13. G. Belingardi, M. P. Cavatorta, and D. S. Paolino, *Int*. *J. Impact*. *Eng*., **35**, 609 (2008).
14. W. A. de Morais, S. N. Monteiro, and J. R. M. d'Almeida, *Compos*. *Struct*., **70**, 223 (2005).
15. M. Chircor, R. Dumitrache, and L. Dumitrache Cosmin, "Proc. of the 3rd International Conference on Maritime and Naval Science and Engineering", Vol. 45, Romania, 2010.
16. A. M. Torki, D. B. Stojanović, I. D. Živković, A Marinković, S. D. Škapin, P. S. Uskoković, and R. R. Aleksić, *Polym*. *Compos*., **33**, 158 (2012).
17. D. B. Stojanović, M. Zrilić, R. Jančić-Heinemann, I. Živković, A. Kojović, P. S. Uskoković, and R. Aleksić, *Polym*. *Adv. Technol*., **24**, 772 (2013).
18. A. M. Torki, I. Živković, V. R. Radmilović, D. B. Stojanović, V. J. Radojević, P. S. Uskoković, and R. R. Aleksić, *Int*. *J. Mod*. *Phys*. *B*, **24**, 805 (2010).
19. Y. Li, T. Yu, T. Pui, P. Chen, L. Zheng, and K. Liao, *Nanoscale*, **3**, 2469 (2011).
20. S. Zainuddin, T. Arefin, A. Fahim, M. V. Hosur, J. D. Tyson, A. Kumar, J. Trovillion, and S. Jeelani, *Compos*. *Struct*., **108**, 277 (2014).
21. N. V. Padaki, R. Alagirusamy, and B. L. Deopura, *Indian J. Fibre Text*. *Tes*., **33**, 189 (2008).
22. A. Majumdar, B. S. Butola, and A. Srivastava, *Mater*. *Design*., **51**, 148 (2013).
23. M. Sánchez-Soto, A. B. Martínez, O. O. Santana, and A. Gordillo, *J*. *Appl*. *Polym*. *Sci*., **93**, 1271 (2004).
24. P. N. B. Reis, P. Santos, J. A. M. Ferreira, and M. O. W. Richardson, *J*. *Reinf*. *Plast*. *Compos*., **32**, 898 (2013).
25. N. Mortas, O. Er, P. N. B. Reis, and J. A. M. Ferreira, *Compos*. *Struct*., **108**, 205 (2014).
26. P. N. B. Reis, J. A. M. Ferreira, P. Santos, M. O. W. Richardson, and J. B. Santos, *Compos*. *Struct*., **94**, 3520 (2012).
27. P. N. B. Reis, J. A. M. Ferreira, Z. Y. Zhang, T. Benaumer, and M. O. W. Richardson, *Compos*. *Pt. B-Eng*., **46**, 7 (2013).